International Journal of Bifurcation and Chaos
© World Scientific Publishing Company

Local Bifurcations of a Quasiperiodic Orbit

Soumitro Banerjee*
Indian Institute of Science Education & Research–Kolkata, Mohanpur, Nadia-741252, WB, India
soumitro@iiserkol.ac.in

Damian Giaouris
Chemical Process Engineering Research Institute (C.P.E.R.I.), Centre for Research and Technology Hellas (CE.R.T.H.), P.O. Box 60361, 57001 Thermi-Thessaloniki, Greece
Damian.Giaouris@newcastle.ac.uk

Petros Missailidis
School of Electrical, Electronic and Computer Engineering, University of Newcastle upon Tyne, NE1 7RU, UK

Otman Imrayed
School of Electrical, Electronic and Computer Engineering, University of Newcastle upon Tyne, NE1 7RU, UK

Received (to be inserted by publisher)

We consider the local bifurcations that can happen to a quasiperiodic orbit in a 3-dimensional map: (a) a torus doubling resulting in two disjoint loops, (b) a torus doubling resulting in a single closed curve with two loops, (c) the appearance of a third frequency, and (d) the birth of a stable torus and an unstable torus. We analyze these bifurcations in terms of the stability of the point at which the closed invariant curve intersects a "second Poincaré section". We show that these bifurcations can be classified depending on where the eigenvalues of this fixed point cross the unit circle.

Keywords: quasiperiodicity, bifurcation, torus

1. Introduction

We investigate the local bifurcations that can happen to a quasiperiodic orbit (or an ergodic torus) in a 3-dimensional map. In various studies on physical and engineering systems, four different types of orbits resulting from such bifurcations have been reported. These are schematically depicted in Fig. 1, where the black firm lines represent the stable orbits and the red dashed lines represent the unstable invariant closed curves resulting from the bifurcation.

Fig. 1(a) and (b) are said to be torus doublings [Kaneko, 1983], but with the difference that in the first case there are two disjoint loops (and the iterates successively toggle between the two) while in the second case there is a single closed curve with two loops. Such disjoint closed loops have been reported in studies on mechanical vibro-impacting systems [Ding *et al.*, 2004; Luo, 2006], in experiments on molten

*Also with the King Abdulaziz University, Jeddah, Saudi Arabia

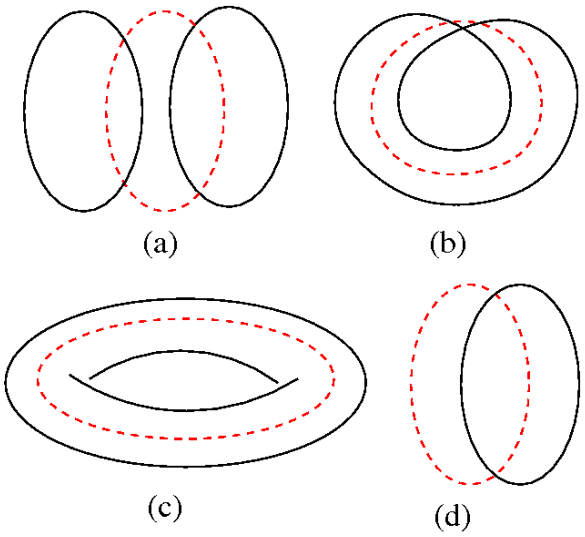

Fig. 1. The four types of behaviors possible in a 3D map, resulting from the local bifurcation of an ergodic torus.

gallium [McKell *et al.*, 1990], and in coupled Chua's circuits [Zhong *et al.*, 1998]. The occurrence of a single closed invarient curve with two loops was reported as early as 1983 [Arneodo *et al.*, 1983], and later in the experiments on vibrating strings [Molteno & Tufillaro, 1990], a circuit with hysteresis element [Sekikawa *et al.*, 2001], 3D Lotka-Volterra model [Bischi & Tramontana, 2010], in a resonant circuit with two saturable inductors [Schilder *et al.*, 2005], in a bimode laser system [Letellier *et al.*, 2007] and in the food chain models used in ecological studies [Osipenko, 2007].

In the case of Fig. 1(c), a third frequency appears and the orbit in *discrete-time* takes the shape of a torus. Following the work of [Ruelle & Takens, 1971; Newhouse *et al.*, 1978], it was believed that such three-frequency quasiperiodic orbits are structurally unstable and should not be expected to occur in nature. But [Grebogi *et al.*, 1983] showed that this behavior can indeed occur in typical dynamical systems, which was subsequently experimentally verified by [Cumming & Linsay, 1988]. Such behavior has also been observed in a vibro-impacting system [Luo *et al.*, 2006]. In this paper we demonstrate the occurrence of stable three-frequency quasiperiodicity in a common power electronic circuit — the current mode controlled boost converter.

In the fourth case (Fig. 1(d)), a stable torus and an unstable torus appear out of nothing, or if the parameter is varied in the opposite direction, they merge and disappear. Such torus-torus collisions have been reported in the quasiperiodically driven logistic map [Heagy & Hammel, 1994] and circle map [Feudel *et al.*, 1995; Kuznetsov *et al.*, 2000, 1998], which give rise to strange nonchaotic attractors.

The purpose of this paper is to relate these observations coming from different branches of science into a single theoretical structure that explains the creation of the orbits shown in Fig. 1 from a stable quasiperiodic orbit. With that purpose, we adopt the approach where a "second Poincaré section" is placed in the discrete-time state space, and we observe the nature of the point at which the closed invariant curve intersects this plane. This approach was earlier proposed by [Kaas-Petersen, 1985, 1987] as a numerical technique to locate the invariant tori, but apparently has not been used by many researchers afterwards. Technically the approach is similar to approximation of the map by an averaged vector field [Schilder *et al.*, 2005; Yoshinaga & Kawakami, 1995; Krauskopf, 2001], and placing a Poincaré section to intersect the continuous trajectory. We apply this approach to analyze the local bifurcation of tori. We report techniques to overcome the problem posed by the fact that there are discrete points filling the drift ring which, in general, do not fall on the second Poincaré section. We report methods to calculate the eigenvalues of the fixed point thus obtained. Using examples from ecological models and power electronics, we show that these bifurcations can be classified depending on where the eigenvalues cross the unit circle.

2. The method of the second Poincaré section

First we consider the mechanisms of the creation of orbits shown in Fig. 1(b), (c), and (d). We shall consider the orbit shown in Fig. 1(a) later in Section 3, because it can be created through local bifurcation of a fixed point.

We start by considering a stable fixed point which undergoes a Neimark-Sacker bifurcation at some parameter value, creating a torus on which the orbit lies. The orbit occurring on the torus could be a mode-locked periodic orbit or a quasiperiodic orbit. In the first case the closed invariant curve is formed by the union of the nodes and the unstable manifolds of the saddle. In the second case the drift ring forms the closed invariant curve. In this paper we consider the second case, where the torus is ergodic in nature, and investigate the possible types of *local* bifurcations such an orbit could undergo as the parameter is varied further.

As a method of investigation, we place a plane transversal to the curve at any arbitrary point (Fig. 2). Let us call it a "second Poincaré section" in the sense that the "first" Poincaré section was used in the continuous-time system to produce the discrete-time map.

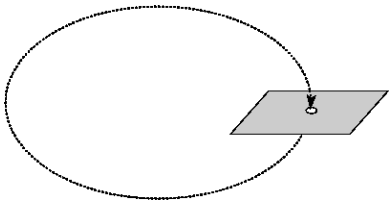

Fig. 2. The "second Poincaré section".

It intersects the continuous curve passing through the points of the orbit at a point. This continuous curve can be viewed as the trajectory of an averaged vector field. Now we can talk about the stability of *this* point of intersection. Since it is a point in the 2D "second Poincaré section", it will have two eigenvalues. Thus it can lose stability in three possible ways, and our proposition regarding the outcome of these bifurcations is as follows.

(1) A complex conjugate pair of eigenvalues may go out of the unit circle. This will create a closed invariant curve around that point. Thus, we have the situation depicted in Fig. 1(c).
(2) An eigenvalue may reach $+1$. This would be like a saddle-node bifurcation of tori, and there must be an unstable closed invariant curve associated with this bifurcation. At this bifurcation they would merge and would go out of existence. If we consider an opposite direction of variation of the parameter, a stable torus and an unstable torus would spontaneously come into existence together at such a bifurcation point. This is the situation depicted in Fig. 1(d).
(3) An eigenvalue goes out of the unit circle through -1 which would lead to period doubling. A period-2 fixed point develops on this second Poincaré section, and the iterates must flip between the points. This gives rise to the situation depicted in Fig. 1(b).

Now we give examples of the three situations.

2.1. *Example of the situation depicted in Fig. 1(c)*

We illustrate the first route using a power electronic circuit—the current mode controlled boost converter, shown in Fig. 3, studied by the authors in [Giaouris *et al.*, 2012]. It is a step-up dc to dc converter commonly used in regulated power supplies. In the power circuit, the switch S is turned on by a free running clock. When the switch S is on, the inductor current i_L rises, and it is switched off when i_L reaches a reference value $I_{\rm ref}$. When the switch is off, the inductor current falls, and the voltage across it adds to the input voltage $V_{\rm in}$, as a result of which a voltage higher than the input voltage appears across the load R (hence the name *boost converter*). The capacitor C helps to maintain this output voltage more or less at a constant level with a small ripple. In order to regulate the output voltage, a reference current signal $I_{\rm ref}$ is generated

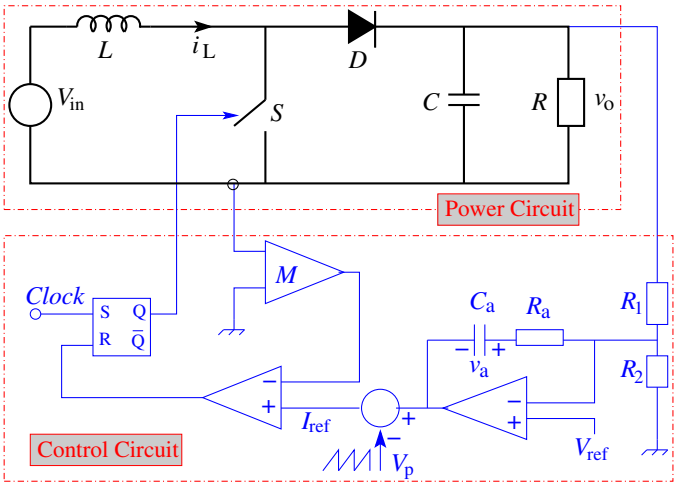

Fig. 3. The schematic circuit diagram of a current mode controlled boost converter.

through output voltage feedback, using a proportional-integral controller and a periodic ramp signal V_p. The *duty ratio* is defined as the duration of the ON period in each clock cycle divided by the duration of the full clock period. The control of the output voltage is exercised by changing the duty ratio in each cycle through the above control logic.

Considering the state vector $x = [i_L\ v_c\ v_a]^T$, the mathematical model is given by [Chen *et al.*, 2007, 2008]:

$$\dot{x} = \begin{cases} A_1 x + B, \text{ for } S = \texttt{ON} \ \text{ and } D = \texttt{OFF} \\ A_2 x + B, \text{ for } S = \texttt{OFF} \text{ and } D = \texttt{ON} \end{cases} \tag{1}$$

with

$$A_1 = \begin{bmatrix} -\frac{r_L + r_T}{L} & 0 & 0 \\ 0 & -\frac{1}{\tau_m(1+k_c)} & 0 \\ 0 & \frac{g}{\tau_a(1+k_c)} & 0 \end{bmatrix}, \quad B = \begin{bmatrix} \frac{1}{L} \\ 0 \\ \frac{g k_d V_{\text{ref}}}{\tau_a V_{\text{in}}} \end{bmatrix}$$

$$A_2 = \begin{bmatrix} -\frac{r_L + r_D}{L} - \frac{r_c}{L(1+k_c)} & -\frac{1}{L(1+k_c)} & 0 \\ \frac{1}{C(1+k_c)} & -\frac{1}{\tau_m(1+k_c)} & 0 \\ \frac{g}{\tau_a(1+k_c)} & \frac{g}{\tau_a(1+k_c)} & 0 \end{bmatrix}$$

and $k_c = r_c/R$, $k_d = R_a/R_1$, $\tau_m = RC$, $\tau_a = R_a C_a$. The nominal parameter values taken in this study are $R = 26\Omega$, $L = 165\mu$H, $r_L = 0.04\Omega$, $C = 150\mu$F, $r_C = 0.03\Omega$, $r_T = 0.055\Omega$, $r_D = 0.01\Omega$, $T = 40\mu$s, $V_{\text{ref}} = 2.5V$, $R_1 = 47k\Omega$, $R_2 = 6.8k\Omega$, $R_a = 10k\Omega$, $C_a = 2.2$nF, $V_p = 0.445$V, $M = 0.3$V/A. We use the input voltage as the variable parameter.

In the normal operating condition of a commercially used converter, the state variables follow a period-1 orbit. But, with the variation of the external parameters like the input voltage or the load resistance, this orbit may become unstable, and other dynamical modes may come into operation. In order to investigate these changes, we fix the load resistance at $R = 25.1\Omega$, and the input voltage is reduced from 3.29V to obtain the bifurcation diagram in Fig. 4. At $V_{\text{in}} \approx 3.28$V, the period-1 behavior undergoes a period doubling bifurcation, followed by a Neimark-Sacker bifurcation occurring on the period-2 orbit. Thus, a two-loop torus is created. As the input voltage is further reduced, at around $V_{\text{in}} = 3.268$V, the torus loses stability, and a third frequency is generated in the system.

Looking at the T-sampled trajectories (Fig. 5) we see that at $V_{\text{in}} = 3.268V$ there are two loops around the two points of the unstable period-2 orbit. When the parameter is reduced to $V_{\text{in}} = 3.266V$, the discrete-time picture itself takes the shape of a torus. The spectrum reveals that at this point a third frequency component is added, and hence the behavior is a three-frequency quasiperiodicity with two loops.

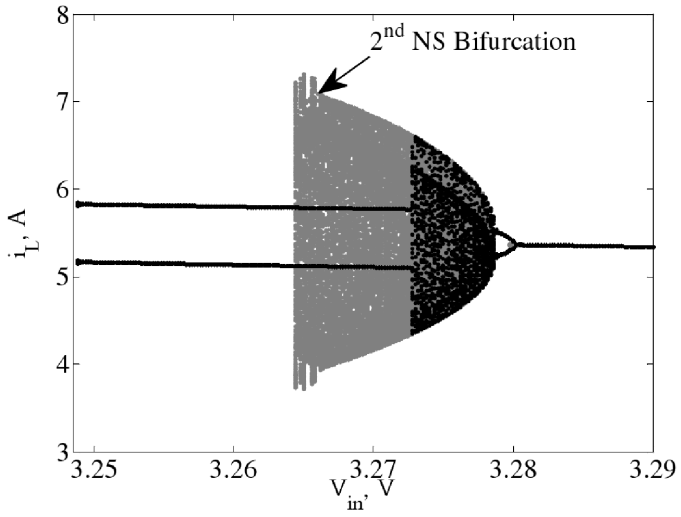

Fig. 4. Bifurcation diagram of the boost converter with the load resistance fixed at $R = 25.1\Omega$, and the input voltage varied as the bifurcation parameter [Giaouris *et al.*, 2012].

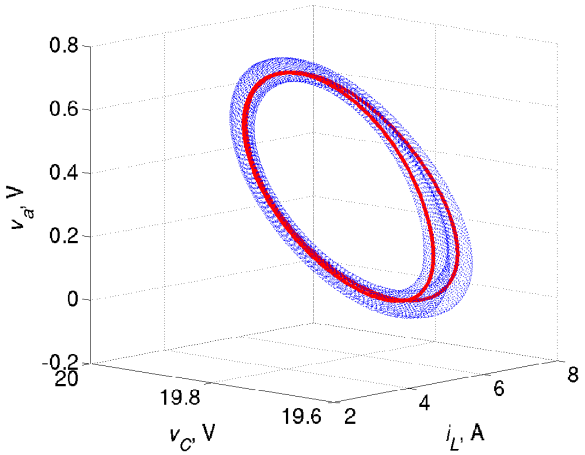

Fig. 5. Trajectories for $V_{\text{in}} = 3.268V$ (in black) and $V_{\text{in}} = 3.266V$ (in grey) sampled every T seconds.

Now we proceed to analyze this event using the method of second Poincaré section. This is a time-driven system with period T, and the object under study in this case is a two-loop torus. In order to concentrate on one of the loops, we sample the trajectory at every $2T$ seconds, thus obtain points on the first Poincaré section that form one loop. Our intention is to study the stability and bifurcation of this quasiperiodic behavior.

Now we place a "second Poincaré section" (say, at $i_L = 5.5A$) to intersect the closed curve on which the points of the $2T$-sampled quasiperiodic orbit lie (Fig. 6). Since the points in general would not fall on this plane, we take three points before and three points after the crossing, and use a spline interpolation to obtain the continuous-time orbit of the averaged vector field. We thus obtain the point where the continuous curve passing through the discrete-time trajectory intersects the second Poincaré section. For the stable quasiperiodic orbit, this procedure yields a fixed point in steady state.

Now we assume that the dynamics on this second Poincaré section, in the neighborhood of the fixed point, is given by a linear equation of the form

$$\mathbf{x}_{n+1} = \mathbf{A}\mathbf{x}_n,$$

where $\mathbf{x}$ represents the deviation from the fixed point. In order to assess the stability of the quasiperiodic orbit, we need to evaluate the Jacobian matrix $\mathbf{A}$ at the fixed point.

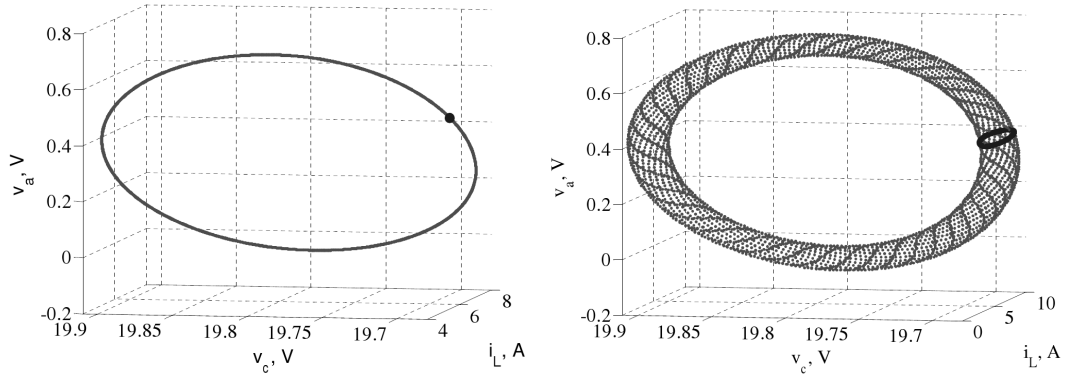

Fig. 6. The twice sampled state space, once at $2T$ and once when $i_l = 5.5$A. Top: when the torus is stable, for $V_{\text{in}} = 3.268V$, bottom: when the 3-frequency torus develops, for $V_{\text{in}} = 3.267V$.

In order to do that, we give a perturbation to the initial condition, and observe the subsequent piercings of the second Poinacré section (shown in Fig. 7). Using the positions of three such piercing points, one can obtain the matrix $\mathbf{A}$, and its eigenvalues. The eigenvalues thus obtained (averaged over a number of such triplets) are listed in Table 1. It is clearly seen that the eigenvalues are complex conjugate, and the magnitude approaches unity as the parameter value of $V_{\text{in}} = 3.268$V is approached.

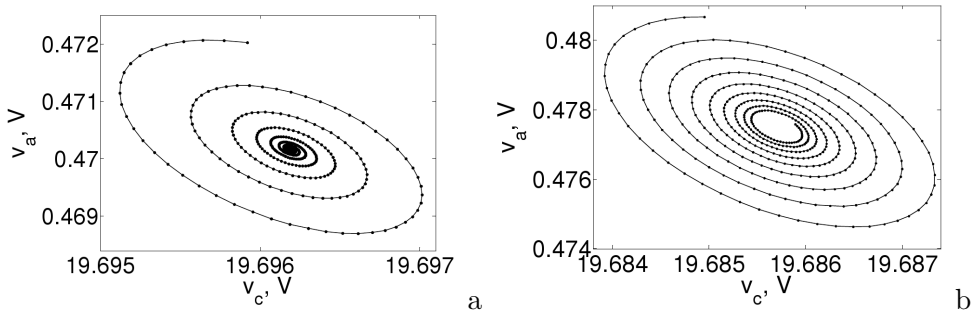

Fig. 7. Second Poincaré points. a) $V_{\text{in}} = 2.271V$, b) $V_{\text{in}} = 2.269V$.

V_{in}	Eigenvalues	Absolute Value
3.271	$0.98146048460 \pm 0.12448292910i$	0.989323345769270
3.270	$0.98444607862 \pm 0.12490543431i$	0.992338374368223
3.269	$0.98770540187 \pm 0.12340583755i$	0.995384830925260
3.268	$0.99119492775 \pm 0.11975828709i$	0.998403441570462

The eigenvalues can also be obtained by another method. If we place the second Poincaré section on a point of the quasiperiodic drift ring, the iterates starting from that point go around the loop and cross the same point 83 iterates later. In order to calculate the stability of the whole quasiperiodic orbit, we have to multiply the state transition matrices across each of these 83 clock cycles.

The system under consideration is nonsmooth, i.e., an orbit would go through multiple operating modes (ON and OFF states of the switch) between consecutive observations of the first Poincaré section. The technique to determine the Floquet multipliers (the eigenvalues of the Jacobian matrix calculated at the fixed point) of such an orbit has been developed recently [Giaouris *et al.*, 2008, 2009, 2007]. The state transition matrix across a whole clock cycle is called a "monodromy matrix" which is the product of the exponential matrices for the ON and OFF periods and the saltation matrices across the switching events [Giaouris *et al.*, 2008, 2009] occurring in that cycle. We calculated the time durations spent in the ON and

OFF phase in each cycle, and thus calculated the monodromy matrix in each cycle. The product of the 83 monodromy matrices gives the local linear approximation around the fixed point on the second Poincaré section. The eigenvalues of this Jacobian matrix gives the stability of the fixed point.

We show in Table 2 the eigenvalues thus obtained, as the parameter is reduced to the bifurcation value. These values are very close to the ones given in Table 1. This shows that even though the procedure is somewhat approximate (since the crossing actually happened somewhere between the 83rd and 84th iterates), it yields reliable results. This happens because in this system the frequencies are different by a few orders of magnitude.

V_{in}	Eigenvalues	Absolute Value
3.271	$0.9822015 \pm 0.1133319i$	0.9887184
3.270	$0.9830253 \pm 0.1449007i$	0.9936473
3.269	$0.9848370 \pm 0.1431570i$	0.9951873
3.268	$0.9931656 \pm 0.1123643i$	0.9995017

Fig. 6 shows that before the onset of this instability, the second Poincaré section could see one point. After the onset of this instability a loop develops. Fig. 7 and Table 2 show that a Neimark-Sacker type bifurcation took place on the already existing torus.

2.2. *Example of the situation depicted in Fig. 1(d)*

The torus-torus collision is also illustrated using the same dc-dc converter system. The bifurcation diagram obtained for a slightly different value of the load resistance is shown in Fig. 8.

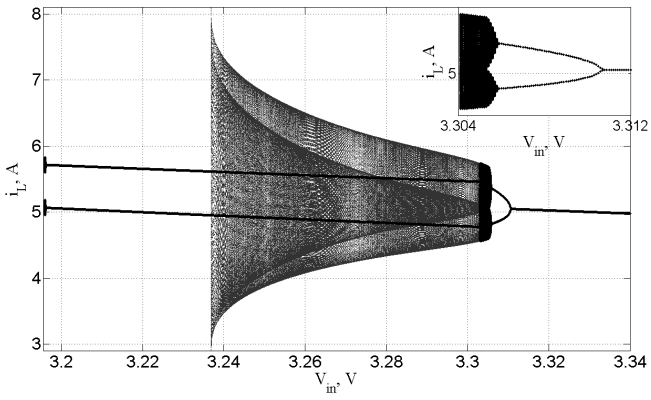

Fig. 8. Bifurcation diagram of the boost converter for $R = 26\Omega$, [Giaouris *et al.*, 2012].

It shows that in the range $V_{\text{in}} = [3.3, 3.2371]$ there are two stable orbits—a period-2 orbit, and a two-loop torus. In fact, there is another attracting behavior where the system "saturates," i.e., the switch remains on. In addition there is an unstable period-1 fixed point, and two unstable tori—one that separates the stable period-2 orbit from the stable torus and one that separates the stable torus from the saturation attractor. These orbits and the basins of attraction are shown in Fig. 9(a).

An interesting event unfolds as the parameter is reduced further, to around $V_{\text{in}} \approx 3.2371$V, when the orbit diverges to the saturation attractor. Our investigation revealed that as the parameter approaches this value, the second stable torus and the unstable torus approach each other and at that parameter value they merge and disappear. After this event, any initial condition outside the first unstable torus diverges to the saturation attractor.

In analyzing this event, we applied the method of second Poincaré section. In this case there is no rotation observed on the second Poincaré section, and the iterates starting from a perturbed initial condition

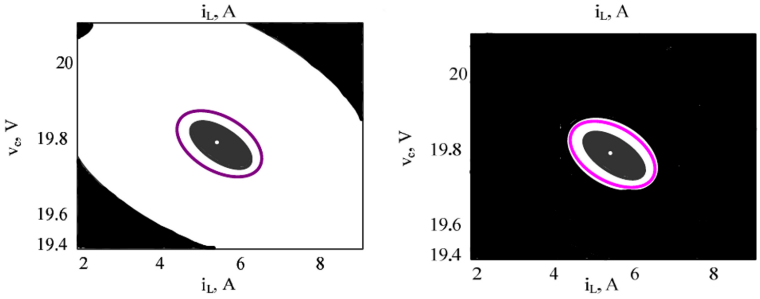

Fig. 9. The basins of attraction observed in the $2T$-return maps. left: $V_{\rm in} = 3.26$: a stable fixed point, a stable torus, the saturation attractor and two unstable tori dividing the basins of attraction; Right: $V_{\rm in} = 3.2371$: the same orbits just before the torus-torus collision.

$V_{\rm in}$	Eigenvalues		
3.28	0.95028922971,	0.94403283208,	−0.95822348419
3.26	0.98728655092,	0.96036314168,	−0.94614257837
3.25	0.99165802082,	0.97522880046,	−0.92296425403
3.24	0.99965802082,	0.98107914455,	−0.84362481946

approach the fixed point along a linear path (which indicates that the eigenvalues should be real and positive). However, close to the bifurcation point, the path on the second Poincaré section becomes wobbly as it approaches the fixed point. This is expected, since the bifurcation occurs not at a single parameter value but over a range of parameter values [Krauskopf, 2001; Schilder *et al.*, 2005].

Starting from a point on the second Poincaré plane, it was observed that the orbit goes through 84 iterations to complete a cycle around the loop. The Jacobian matrix **A** was again calculated as a product of 84 monodromy matrices, and the resulting evolution of the eigenvalues is tabulated in Table 3.

From this table it is clear that one eigenvalue approaches +1 as the parameter approaches the bifurcation value. Thus, this bifurcation is torus equivalent of the saddle-node bifurcation, at which a node and a saddle on the second Poincaré section merge and disappear. In the state space we observe the merging of a stable torus and an unstable torus, and the disappearance of both.

2.3. *Example of the situation depicted in Fig. 1(b)*

The scenario depicted in Fig. 1(b) has not been observed in the power electronic circuit that we have been considering so far. So we consider the 3D Lotka-Volterra model [Gardini *et al.*, 1987; Osipenko, 2007] which is known to exhibit this phenomenon:

$$\begin{aligned} x &\mapsto x + Rx(1 - x - ay - bz) \\ y &\mapsto y + Ry(1 - bx - y - az) \\ z &\mapsto z + Rz(1 - ax - by - z) \end{aligned}$$

For fixed $R = 1, a = 0.5$, it gives a quasiperiodic orbit at $b = -0.65$ (Fig. 10).

We place the second Poincaré section transversal to the curve passing through the drift ring, located at one of the points of the quasiperiodic orbit. In this system, however, the stability of the torus cannot be calculated following the procedure given in the earlier cases because the frequencies involved are not widely different. Since the consecutive iterates on the loop are widely separated, one cannot use spline algorithms to obtain a continuous curve as a close approximation to the drift ring. Moreover, starting from a point on the second Poincaré section, an iterate may not land close to the section after traversing once around the loop. In this case we adopt a slightly different approach to obtain a close approximation of the Jacobian matrix.

We define a tolerance of ϵ around the second Poincaré section. Then, starting from a point on that plane, we continue to iterate the map until a point falls within that tolerance range of the second Poincaré

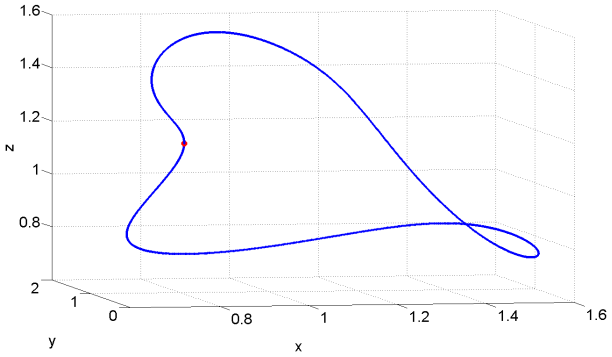

Fig. 10. The quasiperiodic orbit in the 3D Lotka-Volterra system at $b = -0.65$. The second Poincaré secion was placed at the point shown by the red dot. (color online)

section. Suppose the orbit goes through n number of iterations before it crosses this plane again, and the orbit goes around the loop k times before an iterate falls within a distance ϵ of the Poincaré plane. Since in this case the map is given explicitly, we can evaluate the Jacobian matrix at each of these points. We obtain the product of nk Jacobian matrices, obtain the eigenvalues of the resulting matrix, and then take their $1/k$th power to obtain the eigenvalues of the fixed point on the second Poincaré section.

For $b = -0.65$ we obtained the quasiperiodic orbit by simulation, and located the second Poincaré section transversal to the loop at the point $[1.29463267\ 1.19172558\ 0.82794044]^T$. We found that the iterates starting from that point go around the loop 9 times before falling close to the second Poincaré section. The procedure outlined above gives:

$$J = \begin{bmatrix} -0.0013509647 & 0.1249247884 & 0.0077209463 \\ 0.6561635554 & -0.3919617065 & -0.6805223291 \\ -0.5800070664 & 0.2129218475 & 0.5947387092 \end{bmatrix}$$

Its eigenvalues are 0.52038750, -0.31896146, and 0. Hence the eigenvalues of the fixed point on the second Poincaré section are $0.52038750^{1/9} = 0.9299953$, and $-0.31896146^{1/9} = -0.88076450$ (ignoring the zero eigenvalue).

Table 4 gives the eigenvalues calculated this way, as the parameter b is varied. It shows that, as the parameter is reduced, the second eigenvalue approaches -1, and subsequently we observe the "loop-doubling," as shown in Fig. 11. Note that the calculation of the eigenvalues by the above method is prone to numerical errors which tend to build up with the number of cycles around the loop. So one should give more weightage to the *trend* rather than the exact value of the eigenvalues as calculated from the above procedure. Note also that we could proceed only up to $b = -0.657$ at which one eigenvalue was -0.9828. As the bifurcation value is approached, the torus began to break up and the calculation became increasingly unreliable.

b	λ_1	λ_2
-0.65	0.9299953	-0.8807645
-0.653	0.9814073	-0.9181398
-0.657	0.9450149	-0.9828535

Even though a close approach to the bifurcation point was not possible, the trend is clear from Table 4: the torus-doubling occurs when an eigenvalue of the fixed point on the second Poincaré section crosses the unit circle on the negative real line. At this point we must point out that the term "torus doubling," as has been used somewhat sloppily in the earlier literature, should exclude a parameter range, say $[\mu_1, \mu_2]$, where the orbit loses hyperbolicity [Schilder *et al.*, 2005]. Our calculation above shows that an eigenvalue of the fixed point on the second Poincaré section for the stable torus approaches -1 as the parameter approaches μ_1, and we see a stable two-loop torus for $\mu > \mu_2$.

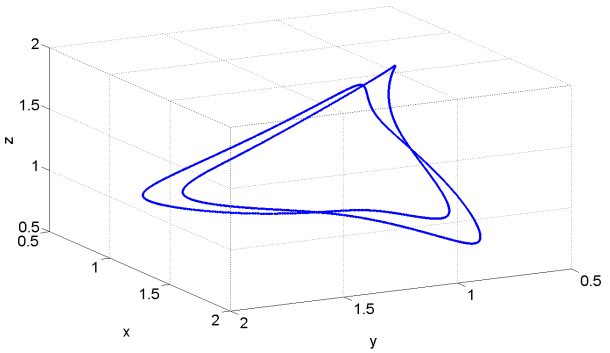

Fig. 11. The two-loop quasiperiodic orbit in the 3D Lotka-Volterra system at $b = -0.658$.

Note that there is an unstable fixed point located at

$$\left(\frac{1}{a+b+1}, \frac{1}{a+b+1}, \frac{1}{a+b+1}\right)$$

inside the torus. For $b = -0.65$, its eigenvalues are 0 and $-0.2647058823 \pm 1.1716814286i$ ($|\lambda| = 1.2012104621$). For $b = -0.657$, when the torus has doubled, the eigenvalues are 0 and $-0.2793594306 \pm 1.1886018887i$ ($|\lambda| = 1.2209898203$). Thus there is no movement of the eigenvalues across the unit circle. This implies that the torus doubling is not a local behavior of the fixed point, and is not reflected by its eigenvalues.

3. Mechanisms of creation of the disjoint loops

In contrast with the cases discussed so far, the situation depicted in Fig. 1(a) can be understood in terms of bifurcations of fixed points (we include this case for the sake of completeness). Ding et al. [Ding *et al.*, 2004] has shown that this situation can come about in two possible ways. Consider the stable fixed point as the starting status.

Route 1: Suppose that the period-1 fixed point has undergone a Neimark-Sacker bifurcation and an invariant closed loop has been created. The unstable fixed point is now located inside the closed invariant curve. It has three eigenvalues. Two are complex conjugate, with magnitude greater than one. The fixed point is stable in the other direction, i.e., the eigenvalue has magnitude less than one. Now suppose this eigenvalue goes out of the unit circle through -1. As a result, the centre of the closed invariant curve will split into two points, which must result in the closed invariant curve also splitting into two disjoint closed curves. This pathway is illustrated in Fig. 12.
Route 2: The fixed point period doubles, i.e., one of the eigenvalues becomes -1. A stable period-2 cycle is created. Each of these period-2 points has three eigenvalues. Suppose that two of the eigenvalues are complex conjugate, thus there is incoming spiralling motion around the two points. Now consider the situation where these complex eigenvalues go out of the unit circle. The Neimark-Sacker bifurcation of the already period-doubled orbit would create a pair of disjoint closed loops (see Fig. 13).

Thus, the creation of two disjoint loops can occur through two sequences: (a) period doubling followed by Neimark-Sacker bifurcation, and (b) Neimark-Sacker bifurcation followed by period doubling.

In fact, an example of the period-doubling–Neimark-Sacker route can be seen in the boost converter example considered in this paper. In the bifurcation diagram of Fig. 8, as the input voltage parameter is reduced, there is a period doubling bifurcation at $V_{\text{in}} = 3.3105$V, followed by a Neimark-Sacker bifurcation of the period 2 orbit at $V_{\text{in}} = 3.3058$V. We find that at the first bifurcation point the duty ratio is 0.8575 and the eigenvalues are -1.0000 and $0.9983 \pm 0.0384i$. At the second bifurcation point ($V_{\text{in}} = 3.3058$V), the duty ratios of the two cycles in a period are 0.9715 and 0.7441, and the eigenvalues of the period-2 orbit are 0.9969, and $0.9996 \pm 0.0754i$ with modulus 1.0000.

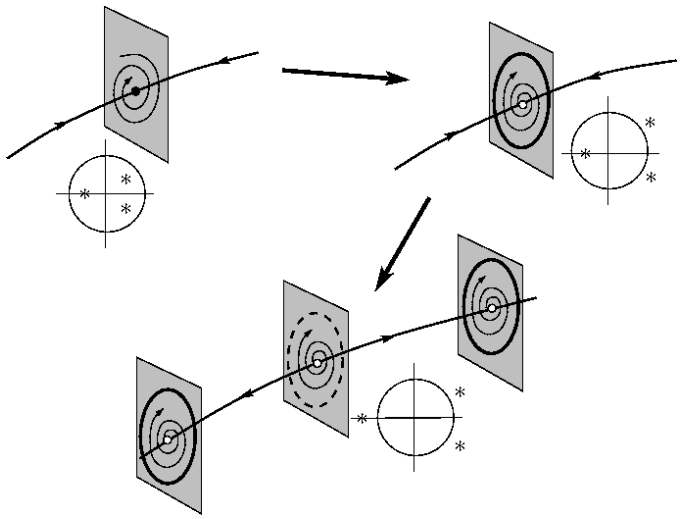

Fig. 12. Illustration of Neimark-Sacker – period-doubling mechanism of creating disjoint closed curves. For each stage, the positions of the eigenvalues of the period-1 fixed point are shown schematically in relation to the unit circle.

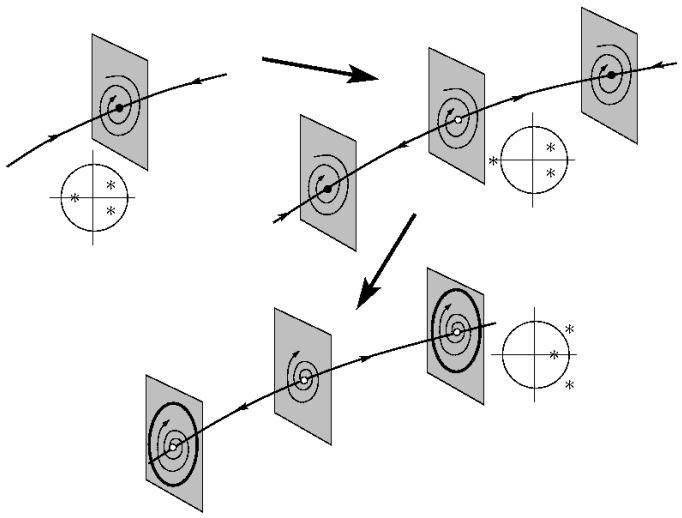

Fig. 13. Illustration of period-doubling – Neimark-Sacker mechanism of creating disjoint closed curves. For the first two stages, the positions of the eigenvalues of the period-1 fixed point are shown schematically in relation to the unit circle, while in last stage the eigenvalues of the period-2 fixed point are shown.

Following the latter bifurcation, the situation in the discrete-time state space is as follows. There is an unstable period-1 fixed point with a stable 2-dimensional manifold and an unstable 1-dimensional manifold. The unstable manifold reaches out to the two unstable period-2 points. Each of these points has a stable 1-dimensional manifold and an unstable 2-dimensional manifold on which the stable quasiperiodic behavior lies. Thus, each point of the period-2 orbit is surrounded by a closed loop representing the torus. The situation is depicted in Fig. 14, obtained by placing an initial condition very close to the stable 2-dimensional manifold of the unstable period-1 fixed point, and observing the iterates.

4. Conclusions

The creation of two disjoint closed curves is the product of local bifurcation of fixed points. There can be two routes: (a) period-doubling followed by Neimark-Sacker bifurcation of the period-2 orbit, (b) Neimark-Sacker bifurcation followed by period-doubling of the unstable period-1 orbit. The other three cases are *not* result of local bifurcation of fixed point. They result from bifurcation of tori.

The local bifurcation of tori can be probed through the method of second Poincaré section, which

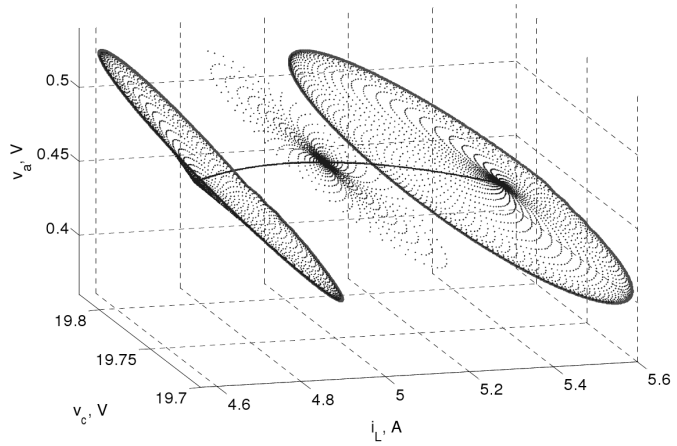

Fig. 14. System's response at $V_{\text{in}} = 3.3032V$, $R = 26\Omega$ starting from an initial condition close to the stable manifold of the period-1 fixed point.

reduces the problem of the stability of a closed invariant curve to the stability of a fixed point. There are three possible routes by which the eigenvalues of such a fixed point can go out of the unit circle.

(1) If an eigenvalue becomes -1, it results in torus doubling producing a single closed invariant curve with two loops;
(2) If an eigenvalue becomes $+1$, it results in the collision between stable and unstable tori, and the disappearance of both;
(3) If a complex conjugate pair of eigenvalues has magnitude 1, it results in the birth of 3-frequency quasiperiodicity.

Acknowledgments

We gratefully acknowledge the discussions with Prof. Laura Gardini, Prof. Bernd Krauskopf, and Prof. Hinke Osinga during the preparation of this paper.

References

Arneodo, A., Coullet, P. H. & Spiegel, E. A. [1983] "Cascade of period doublings of tori," *Physics Letters A* **94**, 1–6.

Bischi, G. & Tramontana, F. [2010] "Three-dimensional discrete-time lotka-volterra models with an application to industrial clusters," *Commun Nonlinear Sci Numer Simulat* **15**, 3000–3014.

Chen, Y., Tse, C. K., Qiu, S. S., Lindenmuller, L. & Schwarz, W. [2008] "Coexisting fast-scale and slow-scale instability in current-mode controlled dc/dc converters: Analysis, simulation and experimental results," *Circuits and Systems I: Regular Papers, IEEE Transactions on* **55**, 3335 –3348.

Chen, Y., Tse, C. K., Wong, S. C. & Qiu, S. S. [2007] "Interaction of fast-scale and slow-scale bifurcations in current-mode controlled dc/dc converters," *International Journal of Bifurcation and Chaos* **17**, 1609–1622.

Cumming, A. & Linsay, P. S. [1988] "Quasiperiodicity and chaos in a system of three competing frequencies," *Physical Review Letters* **60**, 2719–2722.

Ding, W.-C., Xie, J. H. & Sun, Q. G. [2004] "Interaction of hopf and period doubling bifurcations of a vibro-impact system," *Journal of Sound and Vibration* **275**, 27–45.

Feudel, U., Kurths, J. & Pikovsky, A. S. [1995] "The birth of strange nonchaotic attractors," *Physica D* **88**, 176–186.

Gardini, L., Lupini, R., Mammana, C. & Messia, M. G. [1987] "Bifurcations and transitions to chaos in the three-dimensional Lotka-Volterra map," *SIAM J. Appl. Math.* **47**, 455–482.

Giaouris, D., Banerjee, S., Imrayed, O., Mandal, K., Zahawi, B. & Pickert, V. [2012] "Complex interac-

tion between tori and onset of three-frequency quasi-periodicity in a current mode controlled boost converter," *IEEE Transactions on Circuits and Systems-I* **59**, 207–214.

Giaouris, D., Banerjee, S., Zahawi, B. & Pickert, V. [2007] "Control of fast scale bifurcations in power factor correction converters," *IEEE Transactions on Circuits & Systems – II* **54**, 805–809.

Giaouris, D., Banerjee, S., Zahawi, B. & Pickert, V. [2008] "Stability analysis of the continuous conduction mode buck converter via Filippov's method," *IEEE Transactions on Circuits & Systems – I* **55**, 1084–1096.

Giaouris, D., Maity, S., Banerjee, S., Pickert, V. & Zahawi, B. [2009] "Application of Filippov method for the analysis of subharmonic instability in dcdc converters," *Int. J. Circuit Theory & Applications* **37**, 899–919.

Grebogi, C., Ott, E. & Yorke, J. A. [1983] "Are three-frequency quasiperiodic orbits to be expected in typical nonlinear dynamical systems?" *Phys. Rev. Lett.* **51**, 339–342, doi:10.1103/PhysRevLett.51.339.

Heagy, J. F. & Hammel, S. M. [1994] "The birth of strange nonchaotic attractors," *Physica D* **70**, 140–153.

Kaas-Petersen, C. [1985] "Computation of quasi-periodic solutions of forced dissipative systems," *Journal of Computational Physics* **58**, 395–408.

Kaas-Petersen, C. [1987] "Computation, continuation, and bifurcation of torus soultions for dissipative maps and ordinary differential equations," *Physica D* **25**, 288–306.

Kaneko, K. [1983] "Doubling of torus," *Prog. Theor. Phys.* **69**, 1806–1810.

Krauskopf, B. [2001] "Strong resonances and Takens's Utrecht preprint," *Global Analysis of Dynamical Systems*, eds. Broer, H. W., Krauskopf, B. & Vegter, G. (Institute of Physics Publishing, Bristol, UK), pp. 89–108.

Kuznetsov, S., Feudel, U. & Pikovsky, A. [1998] "Renormalization group for scaling at the torus-doubling terminal point," *Physical Review E* **57**, 1585–1590.

Kuznetsov, S. P., Neumann, E., Pikovsky, A. & Sataev, I. R. [2000] "Critical point of tori collision in quasiperiodically forced systems," *Phys. Rev. E* **62**, 1995–2007, doi:10.1103/PhysRevE.62.1995.

Letellier, C., Bennoud, M. & Martel, G. [2007] "Intermittency and period-doubling cascade on tori in a bimode laser model," *Chaos, Solitons and Fractals* **33**, 782–794.

Luo, G. W. [2006] "Hopf-flip bifurcations of vibratory systems with impacts," *Nonlinear Analysis: Real World Applications* **7**, 1029–1041.

Luo, G. W., Chu, Y. D., Zhang, Y. L. & Zhang, J. G. [2006] "Double neimarksacker bifurcation and torus bifurcation of a class of vibratory systems with symmetrical rigid stops," *Journal of Sound and Vibration* **298**, 154179.

McKell, K. E., Broomhead, D. S., Jones, R. & Hurle, D. T. J. [1990] "Torus doubling in convecting molten gallium," *Europhysics Letters* **12**, 513–518.

Molteno, T. C. A. & Tufillaro, N. B. [1990] "Torus doubling and chaotic string vibrations: Experimental results," *Journal of Sound & Vibration* **137**, 327–330.

Newhouse, S. E., Ruelle, D. & Takens, F. [1978] "Quasiperiodicity and chaos in a system of three competing frequencies," *Commun. Math. Phys.* **64**, 35.

Osipenko, G. [2007] *Dynamical Systems, Graphs, and Algorithms* (Springer Verlag, Berlin).

Ruelle, D. & Takens, F. [1971] "On the nature of turbulence," *Commun. Math. Phys.* **20**, 167–192.

Schilder, F., Osinga, H. M. & Vogt, W. [2005] "Continuation of quasi-periodic invariant tori," *SIAM J. Applied Dynamical Systems* **4**, 459–488.

Sekikawa, M., Miyoshi, T. & Inaba, N. [2001] "Successive torus doubling," *IEEE Transactions on Circuits and Systems-I* **48**, 28–34.

Yoshinaga, T. & Kawakami, H. [1995] "Bifurcations and chaotic state in forced oscillatory circuits containing saturable inductors," *Nonlinear Dynamics in Circuits*, eds. Carroll, T. & Pecora, L. (World Scientific Publishing, River Edge, NJ), pp. 89–118.

Zhong, G. Q., Wu, C. W. & Chua, L. O. [1998] "Torus-doubling bifurcations in four mutually coupled chua's circuits," *IEEE Transactions on Circuits and Systems-I* **45**, 186–193.